25 Variation of the Surface to Bulk Contribution to Cluster Properties

Antonis N. Andriotis[1] · *Zacharias G. Fthenakis*[1] · *Madhu Menon*[2]
[1]Institute of Electronic Structure and Laser, FORTH, Heraklio, Crete, Greece
[2]Department of Physics and Astronomy and Center for Computational Sciences, University of Kentucky, Lexington, KY, USA

J. Leszczynski (ed.), *Handbook of Computational Chemistry*, DOI 10.1007/978-94-007-0711-5_25,

Abstract: Recent computer simulations have indicated that there is a linear relationship between the melting and the Curie temperatures for Ni_n ($n \leq 201$) clusters. In this chapter, it is argued that this result is a consequence of the fact that the surface and the core (bulk) contributions to the cluster properties vary with the cluster size in an analogous way. The universal aspect of this result is also discussed. Among the many interesting consequences resulting from this relationship is the intriguing possibility of the coexistence of melting and magnetization. As demonstrated, these conclusions have as their origin the major contribution coming from the melting/magnetization ratio arising from surface effects and appear to overshadow all other contributions. As a result, this can be quantified with approximate methods which are suitable for describing any major surface contribution to a cluster property.

Introduction

As the cluster size increases, the cluster properties evolve toward their bulk counterparts. The understanding of this evolution is of fundamental importance not only from the perspective of basic science but also from the technological viewpoint. At a very approximate level, one can claim that the cluster properties can be described in terms of their surface and core (bulk) contributions and due to the fact that the surface to bulk ratio gets smaller as the cluster size increases. Consequently, it is natural to expect that the cluster properties will evolve to their corresponding bulk-phase ones for large cluster sizes.

As one particular example, we mention the melting temperature of large clusters. According to the proposed model, the following functional relationship for the variation of the melting temperature, $T^{cl}_{melt,N}$, of a cluster as the number N of its atoms increases has been suggested:

$$T^{cl}_{melt,N} = T^{bulk}_{melt} - \delta_{melt} N^{-1/3}, \tag{25.1}$$

where T^{bulk}_{melt} is the melting temperature of the corresponding bulk phase and δ_{melt} is a constant that depends on N (Garcia-Rodeja et al. 1994; Gunes et al. 2000; Lee et al. 2001; Nayak et al. 1998; Qi et al. 2001; Rey et al. 1993; Sun and Gong 1998). Correction terms in $N^{-2/3}$ and N^{-1} powers to the above expression have also been suggested (Doye and Calvo 2001). The term proportional to $N^{-1/3}$ in Eq. 25.1 reflects the surface to bulk contribution to the melting temperature.

Equation 25.1 was found to describe reasonably well the experimental findings in the large-size regime ($N > 500$). However, for clusters of smaller size, (especially for clusters with number of atoms $N \leq 50$), Eq. 25.1 does not ensure a quantitative description of the variation of $T^{cl}_{melt,N}$ with the cluster size (see, e.g., Baletto and Ferrando 2005; Lee et al. 2001; Nayak et al. 1998; Qi et al. 2001). This is because for small clusters, (1) the surface-to-volume contribution to $T^{cl}_{melt,N}$ is very large and (2) is very sensitive to the variations of the surface structure and the cluster geometry (symmetry), as both of these characteristics get altered as the cluster size changes.

Another property that has attracted much interest recently is the one pertaining to the evolution of the magnetic features of the magnetic clusters as the cluster size and temperature increase. This is mainly because of the potential applications of the magnetic grains in fabricating new materials for advanced magnetic storage devices and other applications (Bansman et al. 2005).

Recently, the results of our computer simulations led us to the conclusion that the Curie, $T^{cl}_{C,N}$, and the melting, $T^{cl}_{melt,N}$, temperature of Ni_N clusters consisting of N atoms are linearly

related over a large range of cluster sizes (N ≤ 201), and this relationship is quantified by the following equation (Andriotis et al. 2007) :

$$T^{cl}_{melt,N} = \alpha T^{cl}_{C,N} + \beta, \tag{25.2}$$

where α and β are constants. Least square fitting of our results leads to $\alpha = 0.5414$ and $\beta = 443.82°$K. This relationship was suggested to be related to the ratio of the surface to bulk contributions to the cluster melting as well as to the average magnetic moment per cluster atom, $\bar{\boldsymbol{\mu}}_{i,N}(\mathrm{T})$ $i = 1, ..., N$. It was then claimed that this relationship could be justified within the mean field theory applied separately to the surface and core regions of the cluster (Andriotis et al. 2007).

A cursory thought seems to suggest that any type of direct relationship between $T^{cl}_{melt,N}$ and $T^{cl}_{C,N}$ to be fortuitous since melting and magnetic order seem to reflect completely different aspects of the crystal potential. Therefore, Eq. 25.2 cannot be considered as one which reestablishes a valid physical relationship between these two cluster properties.

Furthermore, the variation of both $T^{cl}_{melt,N}$ and $T^{cl}_{C,N}$ with the cluster size constitute separate distinct and complicated projects for both theory and experiment. This is because significant contributions to both of these physical quantities have their origin in surface as well as cluster-core (bulk) effects which, at first look, affect $T^{cl}_{melt,N}$ and $T^{cl}_{C,N}$ differently. These contributions include: the effects of the cohesive energy, the shape (symmetry), the size, the surface to bulk ratio, the surface tension, the temperature of the cluster, etc.

In early reports, it was found that $T^{cl}_{melt,N}$ is usually smaller than the corresponding bulk value. Of interest is the result applied for large enough spherical clusters of radius R:

$$T^{cl}_{melt,N}/T^{bulk}_{melt} = 1 - k_m/R \tag{25.3}$$

where k_m is a material-dependent constant (see, e.g., Buffat and Borel 1976 and references therein). A similar expression describing the variation of the Curie temperature with the cluster size was also found within the phenomenological Landau–Ginsburg–Devonshire theory (Huang et al. 2000), i.e.,

$$T^{cl}_{C,N}/T^{bulk}_{C} = 1 - k_c/R \tag{25.4}$$

Use of Eqs. 25.3 and 25.4 gives the following values for α and β in Eq. 25.2:

$$\alpha = \frac{k_c}{k_m}\frac{T^{bulk}_C}{T^{bulk}_{melt}} \tag{25.5}$$

and

$$\beta = T^{bulk}_C - \alpha T^{bulk}_{melt} = \left(1 - \frac{k_c}{k_m}\right) T^{bulk}_C. \tag{25.6}$$

Diep and collaborators (Diep et al. 1989) using Monte Carlo simulations studied the effect of the magnetic interactions on the melting temperature of a cluster. Although their investigation was limited to very small clusters M_N, (N ∈ [7,17]) of transition metals M, however, the conclusions they arrived at are very important. In particular, among others, they have found that the incorporation of the magnetic interactions leaves the cluster structure unchanged. However, magnetic interactions lead to sharper peaks in the specific heat (and, therefore, to more precise determination of melting and Curie temperatures), a slight increase in the melting temperature, and a slight cluster-volume contraction (magnetostriction). After examining more carefully the results of Diep et al. (1989) (included in their Fig. 12), we find that the relation of $T^{cl}_{melt,N}$ and $T^{cl}_{C,N}$ is more or less linear with the exception of the data of the very small clusters, i.e., for

N ∈ [7,8,9]. The linear relationship between $T^{cl}_{melt,N}$ and $T^{cl}_{C,N}$ was also suggested recently on the basis of semiempirical and approximate phenomenological model descriptions (see Yang and Jiang 2005 and references therein).

All these descriptions support our findings (i.e., ❯ Eq. 25.2), which are based on a firm quantum mechanical model procedure as outlined in the following. In this work, we investigate the implications of such a relationship which seems to specify a universal aspect of the surface contribution to the cluster properties.

The Model

The investigation of clusters of medium and intermediate sizes consisting of transition metal atoms poses a severe challenge in terms of computer capacities and computer time. For this reason, approximate schemes have been employed with most pronounced being those based on empirical classical potentials. However, these models have limited applicability when there is a need to understand more about the electronic structure of these systems and follow its changes as the cluster size increases and approaches the bulk phase. It is thus necessary to use methods with firm ab initio footing while at the same time not sacrificing computational efficiency. One such method is based on the Tight-Binding approximation which we have adopted in our work.

In this section, we discuss briefly the implementation of this approach in order to model the temperature and magnetic features of transition metal clusters. We will firstly give a brief overview of our TB computational scheme that we used for systems at zero temperature. In the following sections, we will describe the generalization of our method enabling the inclusion of magnetic and temperature effects.

Tight-Binding Molecular Dynamics Methodology

The details of our Generalized Tight-Binding Molecular Dynamics (GTBMD) scheme can be found in Andriotis and Menon (1998) and Menon et al. (1997). The GTBMD method makes explicit use of the nonorthogonality of the orbitals resulting in a transferable scheme that works well in the range all the way from a few atoms to the condensed solid. The scheme also includes d-electron interactions enabling dynamic treatment of magnetic effects in transition metal systems. Here, we give a brief overview.

The total energy U is written in its general form as a sum of several terms (Andriotis and Menon 1998),

$$U = U_{\mathrm{el}} + U_{\mathrm{rep}} + U_0, \tag{25.7}$$

where U_{el} is the sum of the one-electron energies E_n for the occupied states:

$$U_{\mathrm{el}} = \sum_{n}^{occ} E_n. \tag{25.8}$$

In the tight-binding scheme, E_n is obtained by solving the characteristic equation:

$$(\mathbf{H} - E_n\mathbf{S})\mathbf{C}^n = 0, \tag{25.9}$$

where $\mathbf{H}$ is the Hamiltonian of the system and $\mathbf{S}$ the overlap matrix.

The Hellmann–Feynman theorem for obtaining the electronic part of the force is given by Menon et al. (1997),

$$\frac{\partial E_n}{\partial x} = \frac{\mathbf{C}^{n\dagger}\left(\frac{\partial \mathbf{H}}{\partial x} - E^n \frac{\partial \mathbf{S}}{\partial x}\right)\mathbf{C}^n}{\mathbf{C}^{n\dagger}\mathbf{S}\mathbf{C}^n}. \tag{25.10}$$

The total energy expression also derives contributions from ion–ion repulsion interactions. This is approximated by a sum of pairwise repulsive terms and included in U_{rep}. This sum also contains the corrections arising from the double counting of electron–electron interactions in U_{el} (Andriotis and Menon 1998). U_0 is a constant that merely shifts the zero of energy. The contribution to the total force from U_{rep} is rather straightforward. One can then easily do molecular dynamics simulations by numerically solving Newton's equation,

$$m\frac{d^2x}{dt^2} = F_x = -\frac{\partial U}{\partial x} \tag{25.11}$$

to obtain x as a function of time.

Our TBMD scheme for a binary system consisting of elements A and B is based on a minimal set of five adjustable parameters for each pair (A,A), (B,B), and (A,B). These parameters are determined by fitting to experimental data for quantities such as the bond length, the vibrational frequency, and the binding energy of the dimers A_2, B_2, AB; the cohesive energy of the corresponding bulk states of the A, B, AB materials; and the energy level spacing of the lowest magnetic states of the dimer and trimer binary clusters consisting of atoms of A and B type. In the absence of experimental data, we fit to data of small clusters obtained using ab initio methods as described in the following subsection. It is apparent that only five parameters are required in the case of a single species system. The generalization to a system containing more than two kind of atoms is also plausible within this approach.

The fixed set of TB parameters are obtained from the universal scheme proposed by Harrison (1980) suitably scaled with respect to the interatomic distance (Andriotis and Menon 1998).

Collinear Magnetic Effects

In order to calculate the Curie temperature of a magnetic cluster, it is necessary to include non-collinear magnetic effects in our model description. These are introduced by extending our zero temperature (ZT) Tight-Binding Molecular Dynamics (TBMD) approach at the Hubbard-U level of approximation (Andriotis and Menon 1998) which we used to study magnetic clusters in the collinear magnetic approximation. According to this collinear model, an exchange-splitting parameter $s_0^{(i)}$ is introduced which is proportional to the intra-site Coulomb interaction U. This specifies the energy splitting between spin-up and spin-down electrons in the ith-atom in accordance with results obtained by ab initio methods. Thus, within this model, a site-diagonal spin-dependent Hamiltonian term $\mathbf{V}_{spin}^{(i)}$ is introduced which has the form:

$$\mathbf{V}_{spin}^{(i)} = \begin{pmatrix} s_0^{(i)} & 0 \\ 0 & -s_0^{(i)} \end{pmatrix} \tag{25.12}$$

In this model, it is assumed that all atomic magnetic moments (MMs) (of the cluster atoms) are collinear to the z-axis of a local xyz-system assigned to the ith cluster-atom.

The generalization of this model to include non-collinear effects is achieved in three steps. In the first step, we include the randomness in the directions of the atomic MMs. In the second, we include the spin-orbit interaction, and in the third, we include the temperature effects. For the sake of completeness, we briefly discuss this generalization in the following.

Step 1: Inclusion of Randomness in the Direction of the Atomic Magnetic Moments

In the first step, it is assumed that the deviation of the direction of the MM, $\boldsymbol{\mu_i}$, of the ith cluster-atom from the Z-axis of the global coordinate system XYZ is specified by the polar angles (θ_i, ϕ_i) defined with respect to this XYZ system. As a result, the potential $\mathbf{V}_{spin}^{(i)}$, originally defined in the local coordinate system xyz of the ith atom, is transformed to its expression $\mathbf{V}_{spin}^{(i),global}$ in the global system XYZ as follows (Anderson and Hasegava 1955; Uhl et al. 1994):

$$\mathbf{V}_{spin}^{(i),global} = \Xi^{\dagger}(\theta_i, \phi_i)\mathbf{V}_{spin}^{(i)}\Xi(\theta_i, \phi_i), \tag{25.13}$$

where $\Xi(\theta_i, \phi_i)$ is the standard spin-1/2-rotation matrix :

$$\Xi(\theta_i, \phi_i) = \begin{pmatrix} e^{i\phi_i/2}\cos\theta_i/2 & e^{-i\phi_i/2}\sin\theta_i/2 \\ -e^{i\phi_i/2}\sin\theta_i/2 & e^{-i\phi_i/2}\cos\theta_i/2 \end{pmatrix} \tag{25.14}$$

It is assumed that the Z-axis of the global system can be arbitrarily chosen, and a usual choice is to take Z in alignment with the easy axis of the system.

Step 2: Inclusion of Spin-Orbit Interaction

In the second step, we introduce the Spin-Orbit (SO) interaction, $\mathrm{V}_{SO}^{(i)}$, in the ith-atom within the **L**–**S** coupling scheme, i.e., $V_{SO}^{(i)} = -\lambda^{(i)}\mathbf{L}^{(i)} \cdot \mathbf{S}^{(i)}$ where, $\lambda^{(i)}$ is the spin-orbit coupling constant for the ith-atom, $\mathbf{L}^{(i)}$ its orbital angular momentum along the Z-axis, and $\mathbf{S}^{(i)}$ its total spin in the direction of $\boldsymbol{\mu_i}$.

Details of the implementation of the Spin-Orbit interaction within our TBMD method have been reported elsewhere (Andriotis and Menon 2004).

In the presence of a magnetic field, **B** (assumed to be along the direction specified by the polar angles (θ_0, ϕ_0) with respect to XYZ-system), the atomic MMs of the cluster-atoms tend to become parallel to the direction of **B**. The average projection of the MMs of the cluster-atoms, μ_{cl}, along the direction of **B** (which is the experimentally measured quantity) is,

$$\mu_{cl} = \frac{1}{N_{cl}}\left|\sum_{i}^{N_{cl}} \mu_i \cos\gamma_i\right|, \tag{25.15}$$

where N_{cl} is the number of cluster-atoms and $\cos\gamma_i = \cos\theta_0\cos\theta_i + \sin\theta_0\sin\theta_i\cos(\phi_0 - \phi_i)$.

In a different formulation within the Hubbard-U model approximation to the *e-e* correlations, the spin-mixing interaction may be derived from a Coulomb-type Hamiltonian term of the form (Kato and Kokubo 1994; Ojeda et al. 1999): $\mathbf{V}_{smix} = -U\sum_{l\sigma}\rho_{l\sigma,l\bar{\sigma}}c_{l\bar{\sigma}}^{\dagger}c_{l\sigma}$, where $c_{l\sigma}^{\dagger}$ $(c_{l\sigma})$ is the creation (annihilation) operator for an electron with spin σ at site l and $\rho_{l\bar{\sigma},l\sigma}$ denote

the electron density matrix elements, i.e., $\rho_{l\sigma,l\bar{\sigma}} =< c^{\dagger}_{l\bar{\sigma}} c_{l\sigma} >$. It can be easily verified that the Hamiltonian term $\mathbf{V}_{smix}$ is equivalent to that given by Eq. 25.13, i.e., $\mathbf{V}^{(i),global}_{spin}$.

Evaluation of the TB representation of the SO-interaction

In order to proceed with the evaluation of the TB matrix elements of the SO-interaction, we write the SO-term as

$$\mathbf{S} \cdot \mathbf{L} = L_x S_x + L_y S_y + L_z S_z \tag{25.16}$$

and compute the matrix elements with respect to the basis set. We are using a basis set of atomic orbitals $y_{ilm\sigma}(\mathbf{r})$, where the index i specifies the atom on which the atomic orbital (AO) is centered, l specifies the angular momentum, m is used to count the various d-orbitals (i.e., d_{xy}, d_{xz}, d_{yz}, $d_{x^2-y^2}$, d_{z^2}), and σ denotes the spin. In terms of a linear superposition of these basis functions, the single electron wave functions take the form

$$\Psi_{i\sigma}(\mathbf{r}) = \sum_{l,m} C_{ilm\sigma}\, y_{ilm\sigma}(\mathbf{r}), \tag{25.17}$$

where $C_{ilm\sigma}$ denote the coefficients which are to be determined from the diagonalization of the Hamiltonian.

The spin operators of Eq. 25.16 refer to the global system and care has to be exercised as they act on the local spin states, the latter related with the former according to Eqs. 25.13 and 25.14. For example,

$$<\uparrow'_i |S_x| \downarrow'_i>= \frac{1}{2} \cos\phi_i \sin\theta_i, \tag{25.18}$$

where the prime indicates the local functions and $\uparrow, \downarrow$ indicate spin-up and spin-down states, respectively.

The matrix elements of the orbital angular momentum operators are obtained by operating on the angular part of the wave functions which, in our TBMD formalism are described by the Cubic harmonics. As an example, we write down the expression of the average value of the z-component of the orbital magnetic moment, L_z, in terms of its matrix elements :

$$< L_z >= \sum_{i\sigma} \int d\mathbf{r} \Psi^{\star}_{i\sigma}(\mathbf{r}) L_z \Psi_{i\sigma}(\mathbf{r}) \tag{25.19}$$

or

$$< L_z >= \sum_{\sigma} \sum_{i}^{occ} \sum_{l,m} \sum_{l'm'} C^{\star}_{ilm\sigma} C_{il'm'\sigma} \int d\mathbf{r} y^{\star}_{ilm\sigma}(\mathbf{r}) L_z y_{il'm'\sigma}(\mathbf{r}) \tag{25.20}$$

Assuming orthogonality of AOs centered at different atoms, and orthonormal basis functions centered at one particular atom, we finally obtain the following expression for the d-orbital contribution to the orbital magnetic moment $< L^d_z >$:

$$< L^d_z >= \sum_{\sigma} \sum_{i}^{occ} \sum_{l=2} \sum_{mm'} \Delta^{il}_{mm'} C^{\star}_{ilm\sigma} C_{ilm'\sigma} \tag{25.21}$$

where $\Delta^{il}_{mm'}$ are constants easily calculated by applying the relation:

$$L_z Y_{lm} = m Y_{lm} \tag{25.22}$$

where Y_{lm} are the spherical harmonics. For example, a straightforward calculation of the constants $\Delta^{il}_{mm'}$ shows that the only nonzero matrix elements of L_z are the following:

$$< d_{x^2-y^2}|L_z|d_{xy} >= -2i \tag{25.23}$$

and

$$< yz|L_z|zx >= -i \tag{25.24}$$

Combining the above, we construct the spin-dependent TB-representation of the SO-interaction term and add this to the other Hamiltonian terms.

Step 3: Inclusion of Temperature Effects

In the third step, our ZT-TBMD method has been extended by incorporating the *Nose*-bath (Nose 1984) and the Multiple Histogram approximations (Fanourgakis et al. 1997), so as to be applicable to cluster studies at finite temperatures in an efficient way (Andriotis et al. 2006, 2007; Fthenakis et al. 2003). This generalization allows one to calculate the caloric curve for the cluster and use this to study the effect of temperature on the structural, electronic, and magnetic properties of transition metal clusters and binary systems containing transition metal and semiconductor atoms. The method has been used to study the variation of structural and magnetic properties with temperature as well as to obtain the caloric curves of the Ni-clusters (Andriotis et al. 2006, 2007; Fthenakis et al. 2003).

Upon thermalization at temperature T, a cluster can be described by the canonical probability distribution function of total energy, $P_T(E)$, which specifies the probability that the system will be found in the energy interval $[E, E+\Delta E]$ at the specified temperature T. The distribution function corresponding to this temperature, within the canonical ensemble description, is (see Fanourgakis et al. 1997; Schmidt et al. 1997 and references therein):

$$P_T(E) = \frac{n_T(E)}{N_T} = \frac{[\Delta\Gamma(E)]\, e^{-E/k_B T}}{Z_T} \quad , \tag{25.25}$$

where n_T(E) is the number of states in the energy interval $[E, E+\Delta E]$, N_T is the total number of accessible states, k_B is Boltzmann's constant, $\Delta\Gamma(E)$ the number of all the different states with energy in the interval $[E, E+\Delta E]$ (i.e., given by $Z_T = \sum_{E_i} \exp(-\beta E_i) = \sum_i \Delta\Gamma(E_i) \exp(-\beta E_i)$) and Z_T the partition function at temperature T.

A molecular dynamics (MD) simulation at a given temperature T provides numerical values for $n_T(E)$ at every accessible energy E. Having obtained these, we make use of the proposed Multiple Histogram Method (MHM) (Weerasinghe and Amar 1993), and obtain the partition functions Z_{T_j} for a finite set of temperatures T_j, $j = 1, ..., M$ (M ≈ 200) and the entropy terms $S(E_i) = k_B \ln[\Delta\Gamma(E_i)]$ (within an additive constant) for a much larger set of energy values E_i, $i = 1, ..., N$ (N ≈ 6,000) (Weerasinghe and Amar 1993).

Having obtained the quantities n_T(E), Z_T(E) and S_T(E), we can then describe all the thermodynamic properties of the clusters and, in particular, the variation with temperature of their structural, electronic, and magnetic properties.

Computational Approach

The computation of the magnetic features of the clusters is performed within the above described non-collinear TBMD scheme as this allows for a full quantum MD relaxation of systems containing several hundred transition metal atoms while incorporating magnetic effects dynamically. More specifically, it includes: (1) *e-e* correlation effects at the Hubbard-U approximation (Andriotis and Menon 1998), (2) the spin-orbit interaction (in the $\mathbf{L}\cdot\mathbf{S}$ approximation), and (3) non-collinear magnetic effects (Andriotis and Menon 1998, 2004). Furthermore, the effect of temperature (Andriotis et al. 2006; Fthenakis et al. 2003) is included in the formalism while making use of the full *s*, *p*, *d* basis set and contains many unique features that make it ideally suited for the treatment of transition metal (TM) and semiconducting materials. For large-scale simulations we have developed a parallel algorithm that enables molecular dynamics simulations of systems containing atoms in excess of a thousand. This method is more accurate than the order-N methods that are being used at present to treat systems of these sizes. The successful application of our collinear TB scheme (see, e.g., Andriotis et al. 1998, 1999, 2000; Lathiotakis et al. 1996) guarantees similar success for the present generalization as well. Finally, we also mention that this approach has been suitably adapted in order for exclusive use in studying the transport properties (based on our computational codes as described in Andriotis and Menon 2001; Andriotis et al. 2002).

While the TBMD computational approach generalized in such a way is suitable for calculating the magnetic properties of the clusters (of a specific geometry), its use for relaxing the structure of particularly large clusters at nonzero temperatures has been found inefficient due to the extreme computational complexity. This is because the thermodynamic equilibration of a crystal requires sufficiently long MD relaxation time (of the order of 2–6 nanoseconds which is translated into 10–40 million MD steps with each step being of the order of a femtosecond).

In order to make our computations feasible, we firstly reach the thermodynamic equilibrium at each temperature using the classical Sutton–Chen interatomic potential (Sutton and Chen 1990) appropriately fitted to the TBMD results (Fthenakis et al.). It should be noted that for Ni, the classical Sutton–Chen potential (Sutton and Chen 1990) was found to give results closer in agreement with our TBMD method than any other classical potentials in use for Ni (Erkos 2001; Fthenakis et al.). While reaching the thermodynamic equilibrium, we apply our generalized TB formalism every 100 time-steps in order to calculate the MM of the cluster. In the MM calculation, the structure of the cluster is assumed frozen (as obtained within the classical potential approach at that particular time step), and the calculation of the MM of the cluster is repeated for a large number, $N_{ran}^{(i)}$, of atomic *spin configurations* taken randomly over the *ith-structural configuration* ($N_{ran}^{(i)} \approx 120$–$300$ for every i-time step in the present calculations).

In view of these results, ❯ Eq. 25.15 is generalized as follows:

$$\mu_{cl} = \frac{1}{KN_{cl}} \left| \sum_{i}^{N_{cl}} \sum_{j}^{N_{ran}^{(i)}} \mu_i^j \cos\gamma_i^j e^{-(E_i^j - E_0)/k_B T} \right|, \tag{25.26}$$

under the assumption that each spin configuration contributes to the magnetic state of the *i*th geometric configuration with probability $P_M(E_i^j) = \frac{1}{K} e^{-(E_i^j - E_0)/k_B T}$ where,

$$K = \sum_{j}^{N_{ran}^{(i)}} e^{-(E_i^j - E_0)/k_B T}. \tag{25.27}$$

The index j in Eqs. 25.26–25.27 denotes quantities evaluated at the particular jth random atomic spin configuration of the ith structural configuration of the cluster. E_0 is taken to be the energy of the ferromagnetically aligned atomic-spin configuration. In this way, we take the average over the low-lying spin configurations of the cluster of a particular (frozen) geometric structure (i.e., as calculated at the specific time step). Finally, the thermodynamic average of μ_{cl} given by Eq. 25.26 over the various cluster geometric structures (i.e., time-steps) is obtained with the help of the probability $P_T(E)$ as given by Eq. 25.25.

Having obtained the temperature dependence of the average magnetic moment $\mu_{cl}(T)$ per cluster atom, we proceed with the calculation of the temperature dependence of the specific heat of each cluster by taking the derivative $d\{\mu_{cl}(T)\}^2/dT$ of the corresponding $\mu_{cl}(T)$ curves. Following Gerion et al. (2000), we obtain the Curie temperature $T^{cl}_{C,N}$ for each cluster by locating the maximum of the magnetic contribution to C_V. This is repeated for a number of clusters of various sizes.

Results and Discussion

In the present work, our focus is on the properties of the magnetic transition metal clusters and, in particular, on Ni clusters for which experimental data are available for comparison. Using the procedures discussed above, we have calculated the melting, $T^{cl}_{melt,N}$, and the Curie, $T^{cl}_{C,N}$, temperatures of the Ni_N clusters for $N \leq 201$. These results were discussed recently in Andriotis et al. (2007). The melting temperature $T^{cl}_{melt,N}$ has been derived on the basis of the Lindemann index using the caloric curve as obtained from the classical potential MD simulations. The Curie temperature $T^{cl}_{C,N}$ has been derived according to the quantum mechanical procedure discussed above. Both were found to increase with the cluster size tending to their corresponding bulk values as the size of the clusters increases, in good agreement with the existing experimental data (Andriotis et al. 2007).

The correlation between $T^{cl}_{melt,N}$ and $T^{cl}_{C,N}$ obtained from our results is shown in *Fig. 25-1* by the black solid line. This demonstrates and supports the validity of Eq. 25.2. We discuss the universal aspect of this correlation and the conclusions that can be derived from in the following.

Firstly, it should be noted that the conclusions one can arrive at from the obtained relationship between melting and Curie temperatures of magnetic clusters depend crucially on the accuracy with which cluster melting temperatures are determined. This is a major issue as it has been extensively discussed in the literature (see, e.g., Baletto and Ferrando (2005); Qi et al. (2001); Sun and Gong (1998) and references therein). This is because surface melting of small particles occurs in a continuous manner over a broad temperature range in contradistinction to the melting of the solid-core (bulk-like) which occurs at a specific critical temperature (Garrigos et al. 1989). For this reason, it has been proposed that in order for $T^{cl}_{melt,N}$ to be described quantitatively, the surface effects are usually treated separately from the core effects by introducing the *surface thickness*, t_0, as a free parameter and calculate $T^{cl}_{melt,N}$ by expressing firstly the heat of the cluster fusion in terms of t_0 and the cluster radius (see, e.g., Lai et al. 1996). A more commonly used approach for determining $T^{cl}_{melt,N}$ is by employing the Lindemann's criterion, an approach followed in the present work (Fthenakis et al. 2003). Such a calculation is subject to the limitations and the accuracy of this method. In particular, the so derived melting temperatures depend strongly on the choice of the classical potential used (Andriotis et al. (2007); Fthenakis

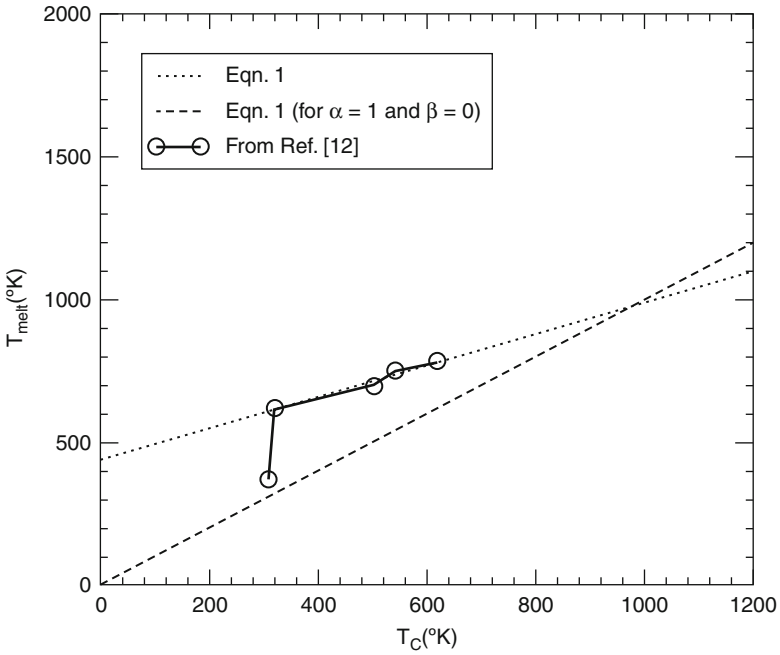

Fig. 25-1

Plot of $T^{cl}_{melt,N}$ as a function of $T^{cl}_{C,N}$ for the Ni_N clusters studied in the present work, N = 43, 80, 147, 177, 201 (*solid line*). The *dotted black line* denoted Eq. 25.2 while and *dashed black line* describes Eq. 25.2 setting $\alpha = 1$ and $\beta = 0$. Points above (below) the *dashed line* have $T_{melt} > T_C$ ($T_{melt} < T_C$) respectively

et al. (2003)). This explains why the reported values for the melting temperature of Ni clusters cover a wide range. Nevertheless, the Sutton–Chen classical potential, employed in the present work for Ni, leads to accurate values for surface energies, vacancy energy, stacking fault energies, and bulk melting temperature in very good agreement with experiment (Qi et al. 2001).

The accuracy of Lindemann's criterion depends also on the steepness of its variation with temperature at phase transition and on the specification of its percentage increase which should be adequate to discriminate surface (partial) from all-cluster melting. In the present case, we assign $T^{cl}_{melt,N}$ to the temperature at which Lindemann's index starts increasing. This allows us to obtain the onset of cluster melting and to derive the melting temperature corresponding to a cluster phase in which unmolten parts with a possible magnetic order are still present.

Similarly, the determination of $T^{cl}_{C,N}$ depends crucially on the accurate location of the maximum of the heat capacity variation with temperature. This was demonstrated in our previous report (Andriotis et al. 2007) when discussing the $T^{cl}_{melt,N}$ and $T^{cl}_{C,N}$ results of Ni_{43} and their deviation from the prediction of Eq. 25.2. Additionally, the surface energy contribution to the free energy of the cluster may be another reason that small cluster temperatures cannot be extrapolated to bulk phase values (Qi et al. 2001).

Following these clarifications, we next discuss some obvious and hidden consequences of Eq. 25.2. One of the first conclusion that can be deduced from these results is that the Curie

temperature, $T^{cl}_{C,N}$, of a magnetic cluster has to follow a size-dependence relationship analogous to that of $T^{cl}_{melt,N}$. That is, if $T^{cl}_{melt,N}$ is given by Eq. 25.1, then $T^{cl}_{C,N}$ has to follow the following equation:

$$T^{cl}_{C,N} = T^{bulk}_{C} - \delta_C N^{-1/3}, \tag{25.28}$$

where δ_C is a constant that may have an N-dependence as δ_{melt}. In fact, assuming the validity of Eqs. 25.1 and 25.28 and taking the ratio between Eq. 25.1 and Eq. 25.28 by parts, we obtain:

$$\frac{T^{cl}_{C,N} - T^{bulk}_{C}}{T^{cl}_{melt,N} - T^{bulk}_{melt}} = \frac{\delta_C}{\delta_{melt}} = \delta_0, \tag{25.29}$$

where δ_0 is a constant which is expected to depend on N. It is apparent that Eq. 25.29 has exactly the form of our Eq. 25.2, suggesting that the N-dependence of the constant δ_0 is very weak.

It is worth noting that the numerical justification of Eq. 25.29 by our results as expressed by Eq. 25.2 cannot ensure that the trends described by Eqs. 25.1 and 25.28 and which are possibly valid for large clusters can be extrapolated to small clusters as well. The conclusion that comes from Eq. 25.2 is that whatever the functional relationship between the melting temperature of a cluster and its size (not necessarily limited to that of Eq. 25.1) is, the functional relationship followed by $T^{cl}_{melt,N}$ should dictate the relationship between the Curie temperature with its size as well. This hypothesis is supported by the results of Diep and collaborators (Diep et al. 1989) who found that the incorporation of the magnetic interactions leaves the cluster structure unchanged, thereby justifying our computational procedure.

One may argue that the use of two noncomparable methods, i.e., that of a classical potential MD simulation for calculating the melting temperature and a quantum mechanical approximation for calculating the magnetic moments and the Curie temperature of a cluster, cannot lead to results that can be correlated. We addressed this issue by fitting the classical Sutton–Chen potential to the data for small clusters in such a way that resulted in TBMD and fitted Sutton–Chen potential simulations giving the same structural properties for small Ni clusters. Obtaining similar structural results by both methods appears to confirm the validity of the classical potential MD simulations for our present purpose.

Furthermore, in order to resolve any reservations and ambiguities about the consistency of our conclusions derived from the use of mutually inconsistent methods in calculating the melting and Curie temperatures, it is demonstrated in the following that a calculation of the melting temperatures within our TBMD approximation is in excellent agreement with the results of the classical potential approximation used in the derivation of Eq. 25.2.

Following exactly the same procedure as the one we used to calculate the average magnetic moment per cluster atom (and from this the Curie temperature) (Andriotis et al. 2007), we calculate the average total energy, $< E_T >$, of each cluster at its thermodynamic equilibrium at a series of temperatures T. An average over N_{ran} random spin configurations over the cluster atoms is taken at each kth time step for N_{cl} time steps (N_{ran} is taken approximately between 100 and 200). Finally, these spin-averaged values are averaged over time. That is,

$$< E_T >= \frac{1}{N_{cl}} \sum_{k=1}^{N_{cl}} \frac{1}{N_{ran}} \frac{\sum_{i=1}^{N_{ran}} E_i^k e^{-(E_i^k - E_0)/k_B T}}{\sum_{i=1}^{N_{run}} e^{-(E_i^k - E_0)/k_B T}}. \tag{25.30}$$

where E_0 is a reference energy (Andriotis et al. 2007). For completeness, it is recalled that

$$E_i^k = \sum_{j\sigma} \varepsilon_{j\sigma}^{i,k} + E_{rep}^{i,k} \tag{25.31}$$

where $\varepsilon_{j\sigma}^{i,k}$ denote the eigenvalues of the TB cluster Hamiltonian and $E_{rep}^{i,k}$, the sum of the repulsive interactions (Andriotis and Menon 1998) of the cluster at the ith random spin configuration and the kth time step. As in the case of the calculation of the Curie temperatures, the averaging process over time in Eq. 25.30 is performed while reaching the thermodynamic equilibrium every 100 time-steps.

In *Figs. 25-2* and *25-3*, we present our TB results for the variation with temperature of $< E_T >$ for the Ni_{147} and Ni_{201} clusters. For Ni_{147}, it is observed that the onset of a phase change appears at $\approx 450^{\circ}$K while the melting starts at $\approx 700^{\circ}$K. For Ni_{201}, the melting takes place

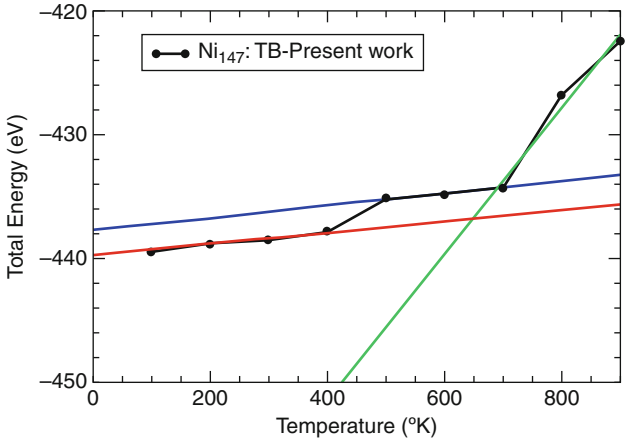

Fig. 25-2
Numerical results obtained within the TBMD method for the variation with temperature of the average total energy of the Ni_{147} cluster. Straight lines are least square fits to portions of the numerical data

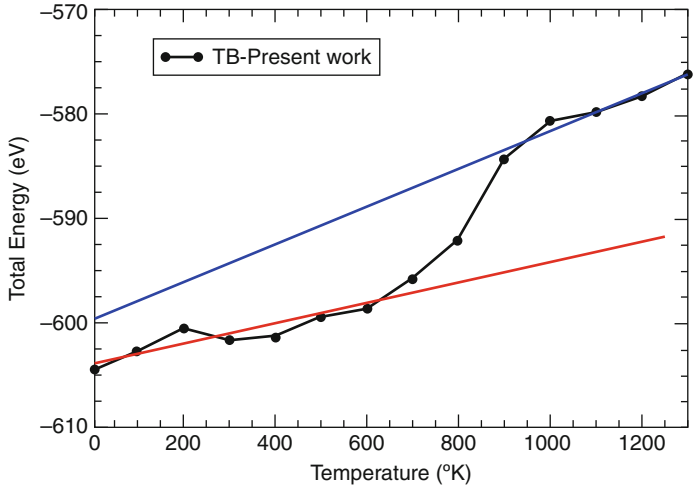

Fig. 25-3
The same as in *Fig. 25-2* but for the Ni_{201} cluster

at ≈ 800°K (taken to be the midpoint of the "parallel" shift of the two linear parts of the thermodynamic curve. The so obtained melting temperatures appear to be in excellent agreement with the results found using the classical potential method and the Lindemann criterion according to which $T^{cl}_{melt,N=147} = 700$°K and $T^{cl}_{melt,N=201} = 780$°K.

Further headway can be made if Eq. 25.2 is taken to be the zeroth-order approximation of a *piece-wise function of N* in analogy to similar findings (Gunes et al. 2000; Qi et al. 2001) for the expression for $T^{cl}_{melt,N}$ given by Eq. 25.1. In this view, the results of Diep et al. (1989) (see Fig. 12 of their work) in the extreme case of very small clusters (N ∈ [7,17]) can lend support to our results and conclusions.

The appearance of the nonzero constant term at the right-hand side of Eq. 25.2 indicates that there is a possibility for $T^{cl}_{C,N}$ to be greater than $T^{cl}_{melt,N}$. In particular, Eq. 25.2 predicts that $T^{cl}_{C,N}$ could be greater than $T^{cl}_{melt,N}$ if

$$T^{bulk}_{C} > T^{cl}_{C,N} > \frac{\beta}{1-\alpha} \quad . \tag{25.32}$$

However, according to our results, the above inequality does not hold for the Ni clusters since $\beta/(1-\alpha) \approx 968$°K, a value much greater than $T^{bulk}_{C} = 631$°K. This is demonstrated in *Fig. 25-1* with the indicated crossing of the dotted and dashed black lines with the former describing Eq. 25.2 and the latter describing the same equation taking $\alpha = 1$ and $\beta = 0$ (i.e., corresponding to the $T^{cl}_{C,N} = T^{cl}_{melt,N}$ case). This incompatibility can be taken as an indication that the functional forms dictated by Eqs. 25.1 and 25.28 are not valid for the entire range of the cluster sizes.

The nonzero value of the constant β has another consequence; it predicts that the ratio $\frac{T^{cl}_{melt,N}}{T^{cl}_{C,N}}$ depends on the cluster size and, in fact, increases as the cluster size decreases. If the variation of $T^{cl}_{melt,N}$ is assumed as given by Eq. 25.1, the predictions of Eq. 25.2 lead to the conclusion that $T^{cl}_{C,N}$ decreases at a slower rate than $T^{cl}_{melt,N}$ as the cluster size decreases and, therefore, the "melting temperatures" of *partially molten clusters* can be found to be lower than the Curie temperatures as Eq. 25.2 implies. However, such a conclusion has to be taken with care as the validity of Eq. 25.1 over the entire range of cluster sizes is not valid.

Conclusion

We have presented results for the variation with the cluster size of the melting and Curie temperatures of Ni_n, n ≤ 201, clusters. Two complimentary methods were used, i.e., the classical MD employing the Sutton–Chen potential and the TBMD for obtaining the melting and the Curie temperatures of the clusters. We have demonstrated that by fitting the classical potential to the results of the TB description in the case of small clusters, we can achieve excellent agreement between the results of the two methods referring to the structural properties and the estimation of the melting temperatures of the clusters.

Our results demonstrate without any ambiguity that the variation of the cluster properties with the cluster size exhibits strong dependence on the ratio of the surface to bulk (core) contributions, the latter appearing to have the same functional dependence on the cluster size for both $T^{cl}_{C,N}$ and $T^{cl}_{melt,N}$.

In view of the established dependence of the melting temperature of a cluster on its surface to volume contribution (as, for example, Eq. 25.1), our conclusion can be interpreted as an

indication of a universal aspect of the surface to volume contribution to the cluster properties. This justifies previous findings based on approximate and semiempirical approximations.

Acknowledgments

The present work is supported by grants from US-DOE (DE-FG02-00ER45817 and DE-FG02-07ER46375).

References

Anderson, P. W., & Hasegava, H. (1955). Considerations on double exchange. *Physical Review, 100*, 675.

Andriotis, A. N., Fthenakis, Z., & Menon, M. (2006). Theoretical study of the effect of temperature on the magnetism of transition metal clusters. *Europhysics Letters, 76*, 1088.

Andriotis, A. N., Fthenakis, Z. G., & Menon, M. (2007). Correlated variation of melting and curie temperatures of nickel clusters. *Physical Review B, 75*, 073413.

Andriotis, A. N., & Menon, M. (1998). Tight-binding molecular-dynamics study of ferromagnetic clusters. *Physical Review B, 57*, 10069.

Andriotis, A. N., & Menon, M. (2001). Greens function embedding approach to quantum conductivity of single wall carbon nanotubes. *Journal of Chemical Physics, 115*, 2737.

Andriotis, A. N., & Menon, M. (2004). Orbital magnetism: Pros and cons for enhancing the cluster magnetism. *Physical Review Letters, 93*, 026402.

Andriotis, A. N., Menon, M., Froudakis, G. E., Fthenakis, Z., & Lowther, J. E. (1998). A tight-binding molecular dynamics study of ni(m)si(n) binary clusters. *Chemical Physics Letters, 292*, 487.

Andriotis, A. N., Menon, M., Froudakis, G. E., & Lowther, J. E. (1999). Tight-binding molecular dynamics study of transition metal carbide clusters. *Chemical Physics Letters, 301*, 503.

Andriotis, A. N., Menon, M., & Froudakis, G. E. (2000). Contrasting bonding behaviors of 3-d transition metal atoms with graphite and c60. *Physical Review B, 62*, 9867.

Andriotis, A. N., Menon, M., & Srivastava, D. (2002). Transfer matrix approach to quantum conductivity calculations in single wall carbon nanotubes. *Journal of Chemical Physics, 117*, 2836.

Baletto, F., & Ferrando, R. (2005). Structural properties of nanoclusters: Energetic, thermodynamic and kinetic effects. *Reviews of Modern Physics, 77*, 371.

Bansman, J., Baker, S. H., Binns, C., Blackman, J. A., Bucher, J. P., Dorantes-Davila, J., Dupuis, V., Favre, L., Kechrakos, D., Kleibert, A., Meiwes-Broer, K. H., Pastor, G. M., Perez, A., Toulemonde, O., Trohidou, K. N., Tuaillon, J., & Xie, Y. (2005). Magnetic and structural properties of isolated and assembled clusters. *Surface Science Reports, 56*, 189.

Buffat, P., & Borel, J. P. (1976). Size effect on the melting temperature of gold particles. *Physical Review A, 13*, 2287.

Diep, H. T., Sawada, S., & Sugano, S. (1989). Melting and magnetic ordering in transition-metal microclusters. *Physical Review B, 39*, 9252.

Doye, J. P. K., & Calvo, F. (2001). Entropic effects on the size dependence of cluster structures. *Physical Review Letters, 86*, 3570.

Erkos, S. (2001). In D. Stauffer (Ed.), *Annual reviews of computational physics* (Vol. IX). World Scientific Publ.

Fanourgakis, G. S., Farantos, S. C., Parneix, P., & Brechignac, P. (1997). An effective transition state for a complex cluster isomerization process: Comparison between anharmonic and harmonic models for $mg^{+}ar_{12}$. *Journal of Chemical Physics, 106*, 4954.

Fthenakis, Z., Andriotis, A. N., & Menon, M. (unpublished).

Fthenakis, Z., Andriotis, A. N., & Menon, M. (2003). Temperature evolution of structural and magnetic properties of transition metal clusters. *Journal of Chemical Physics, 119*, 10911.

Fthenakis, Z., Andriotis, A. N., & Menon, M. (2003). Understanding the structure of metal encapsulated si cages and nanotubes. *Journal of Chemical Physics, 119*, 10911.

Garcia-Rodeja, J., Rey, C., Gallego, L. J., & Alonso, J. A. (1994). Molecular-dynamics study of the structures, binding energies, and melting of clusters of fcc transition and noble metals using the *v*oter and *c*hen version of the embedded-atom model. *Physical Review B, 49*, 8495.

Garrigos, R., Cheyssac, P., & Kofman, R. (1989). Melting for lead particles of very small sizes: Influence of surface phenomena. *Zeitschrift für Physik D, 12*, 497.

Gerion, D., Hirt, A., Billas, I. M. L., Chatelain, A., & de Heer, W. A. (2000). Experimental specific heat of iron, cobalt, and nickel clusters studied in a molecular beam. *Physical Review B, 62*, 7491.

Gunes, B., & Erkoc, S. (2000). Melting and fragmentation of nickel nanparticles: Molecular-dynamics simulations. *International Journal of Modern Physics, 11*, 1567.

Harrison, W. (1980). *Electronic structure and properties of solids*. San Francisco: W. H. Freeman.

Huang, H., Sun, C. Q., & Hing, P. (2000). Surface bond contraction and its effect on the nanometric sized lead zirconate titanate. *Journal of Physics: Condensed Matter, 12*, L127.

Kato, M., & Kokubo, F. (1994). Partially antiferromagnetic state in the triangular hubbard model. *Physical Review B, 49*, 8864.

Lai, S. L., Guo, J. Y., Petrova, V., Ramanath, G., & Allen, L. H. (1996). Size-dependent melting properties of small tin particles: Nanocalorimetric measurements. *Physical Review Letters, 77*, 99.

Lathiotakis, N. N., Andriotis, A. N., Menon, M., & Connolly, J. (1996). Tight binding molecular dynamics study of ni clusters. *Journal of Chemical Physics, 104*, 992.

Lee, Y. J., Lee, E. K., Kim, S., & Nieminen, R. M. (2001). Effect of potential energy distribution on the melting of clusters. *Physical Review Letters, 86*, 999.

Menon, M., & Subbaswamy, K. R. (1997). Nonorthogonal tight-binding molecular-dynamics scheme for silicon with improved transferability. *Physical Review B, 55*, 9231.

Nayak, S. K., Khanna, S. N., Rao, B. K., & Jena, P. (1998). Thermodynamics of small nickel clusters. *Journal of Physics Condensed Matter, 10*, 10853.

Nose, S. (1984). A unified formulation of the constant temperature molecular dynamics methods. *Journal of Chemical Physics, 81*, 511.

Ojeda, M. A., Dorantes-Davila, J., & Pastor, G. (1999). Noncollinear cluster magnetism in the framework of the hubbard model. *Physical Review B, 60*, 6121.

Qi, Y., Cagin, T., Johnson, W. L., & Goddard, W. A. (2001). Melting and crystallization in ni nanoclusters: The mesoscale regime. *Journal of Chemical Physics, 115*, 385.

Rey, C., Gallego, L. J., Garcia-Rogeja, J., Alonso, J. A., & Iniguez, M. P. (1993). Molecular-dynamics study of the binding energy and melting of transition-metal clusters. *Physical Review B, 48*, 8253.

Schmidt, M., Kusche, R., Kronmuller, W., von Issendorff, B., & Haberland, H. (1997). Experimental determination of the melting point and heat capacity for a free cluster of 139 sodium atoms. *Physical Review Letters, 79*, 99.

Sun, D. Y., & Gong, X. G. (1998). Structural properties and glass transition in al_n clusters. *Physical Review B, 57*, 4730.

Sutton, A. P., & Chen, J. (1990). Long-range finnis-sinclair potentials. *Philosophical Magazine Letters, 61*, 139.

Uhl, M., Sanrdatskii, L. M., & Kubler, J. (1994). Spin fluctuations in γ-fe and in fe_3pt invar from local-density-functional calculations. *Physical Review B, 50*, 291.

Weerasinghe, S., & Amar, F. G. (1993). Absolute classical densities of states for very anharmonic systems and applications to the evaporation of rare gas clusters. *Journal of Chemical Physics, 98*, 4967.

Yang, C. C., & Jiang, Q. (2005). Size and interface effects on critical temperatures of ferromagnetic, ferroelectric and superconductive nanocrystals. *Acta Materialia, 53*, 3305.